We are IntechOpen, the world's leading publisher of Open Access books Built by scientists, for scientists

6,900
Open access books available

185,000
International authors and editors

200M
Downloads

Our authors are among the

154
Countries delivered to

TOP 1%
most cited scientists

12.2%
Contributors from top 500 universities



WEB OF SCIENCE™

Selection of our books indexed in the Book Citation Index in Web of Science™ Core Collection (BKCI)

Interested in publishing with us?
Contact book.department@intechopen.com

Numbers displayed above are based on latest data collected.
For more information visit www.intechopen.com



Chapter 10

Wind-Driven Self-Excited Reluctance Generator for Rural Electrification

Ayodeji S.O. Ogunjuyigbe, Temitope R. Ayodele, Bukola B. Adetokun and Adisa A. Jimoh

Additional information is available at the end of the chapter

http://dx.doi.org/10.5772/62738

Abstract

This chapter presents the dynamic performance of an isolated wind-driven self-excited reluctance generator (WDSERG) for rural electrification application. The performances of the machine under conditions of constant wind speed, varying wind speed, constant load, and varying loads are analysed and presented. The modelling and simulation have been carried out using MATLAB-Simulink. A step-wise procedure clearly set forth for the Simulink implementation of the wind-driven machine forms the balance of this work, which can be a good teaching aid. The result shows that with the variations in the connected loads, the output frequency of SERG remains constant, which makes it a good alternative for rural electrification.

Keywords: self-excited reluctance generator, rural electrification, wind speed, MATLAB-Simulink, dynamic performance

1. Introduction

The age-long exploitation of fossil fuel has resulted into attendant global warming, which has become the single largest environmental threat globally. An attempt to mitigate the effects of climate change due to the burning of fossil fuels and to meet the increasing energy demand has informed multi-dimensional researches into the harnessing of renewable energy sources for power generation. Thus, exploration of renewable energy sources such as hydro, solar, wind, and geothermal energies has gained global attention [1, 2].

INTECH
open science | open minds

© 2016 The Author(s). Licensee InTech. This chapter is distributed under the terms of the Creative Commons Attribution License (http://creativecommons.org/licenses/by/3.0), which permits unrestricted use, distribution, and reproduction in any medium, provided the original work is properly cited. CC BY

Distributed generation is also receiving a rapt attention over centralized generation due to cost of transmission, particularly to rural areas which are mostly remote and isolated from the urban regions. The underlying issues involved in such distributed generation includes energy conversion, control, and integration . A number of electrical machines can be used for the electromechanical energy conversion, each with its attendant merits and demerits [3, 4].

The use of self-excited induction generator (SEIG) in isolated wind turbine energy conversion has gained prominence in recent years. This is largely due to its inherent advantages over the conventional synchronous generator, which includes simple, brushless, rugged, and robust construction with squirrel cage rotor, relatively low initial and maintenance cost, self protection against excessive overload, and short-circuit contingencies [5]. In addition, SEIGs require no external direct current (DC) supply for excitation and voltage regulation, and they have better transient performances [6]. On the other hand, the major drawbacks of SEIG are poor voltage and frequency regulations under varying prime mover speed and loading conditions. Its output frequency and generated voltage are dependent on the speed of the prime mover, hence a need for frequency and voltage stabilizing and control circuits, which invariably increases the installation cost [7, 8].

Another self-excited machine that can also provide a good and competitive potential for wind energy conversion for rural electrification is the self-excited reluctance generator (SERG). Three-phase SERG has almost all the advantages of SEIG. An additional advantage of SERG is the fact that it has constant output frequency in spite of varying loading conditions and excitation capacitances. Another desirable advantage of SERG is that of enhanced steady state performances and relatively high efficiency over a wide range of operation [9].

In view of its shortcomings, SEIG suffers in terms of changes in both magnitude and frequency of the generated voltage under various loads. A salient-pole or segmental pole rotor SERG without dc excitation has been proposed to decrease such problem [10].

This chapter therefore focuses on the harnessing of wind energy for electric power generation in rural areas using SERG. A detailed mathematical model of energy conversion with SERG suitable for the dynamic and transient analysis of the machine is presented. The model is utilised to build an investigative simulation tool in the MATLAB-Simulink environment. The advantages of SERG over SEIG are shown in the simulation results.

Also, a typical model of a wind turbine is developed and integrated to that of the SERG to obtain a complete network for the wind-driven self-excited reluctance generator (WDSERG). The complete model was used to simulate the WDSERG. Different scenarios of wind speed and load conditions were investigated to determine the process of voltage build-up and voltage collapse. Simulation results of the SERG driven by a wind turbine are presented in the concluding section of this chapter.

2. Wind turbine model

Wind energy is one of the most prominent renewable energy sources on earth. In recent years, there has been a marked growth in the harnessing of this resource for electricity generation.

http://dx.doi.org/10.5772/62738

The installed power increased from 7.5 GW in 1997 to more than 194 GW in 2010 globally [11]. This brought about a corresponding increase in the size and power ratings of turbines, with rotor diameters of more than 100 m and power ratings ranging from kilowatts to megawatts. The obvious need for off-grid distributed generation is another reason for the increasing demand for the design, construction, and operation of wind energy conversion systems. The mechanical output power of the turbine (in Watts) is given by:

$$P_m = \frac{1}{2} C_p(\lambda, \beta) \rho A v_w{}^3 \tag{1}$$

where C_p is the performance coefficient of the turbine, λ is the tip speed ratio (TSR), β is the blade pitch angle, ρ is density of air in Kg/m^3, A is the turbine swept area in m^2, and v_w is the wind speed in m/s. The performance coefficient (C_p) of the turbine is a measure of how much mechanical power can be derived from the wind, that is, the aerodynamic efficiency of the turbine. It represents the fraction of the wind's kinetic energy that is converted into mechanical energy. It is a function of the tip-speed ratio (λ) and blade pitch angle (β) given by:

$$C_p(\lambda, \beta) = C_1 \left(\frac{C_2}{\lambda_1} - C_3 \beta - C_4 \right) e^{\frac{-C_5}{\lambda_1}} + C_6 \lambda \tag{2}$$

Where

$$\lambda_1 = \frac{\left(\beta^3 + 1\right)\left(\lambda + 0.08\beta\right)}{\beta^3 - 0.028\beta - 0.035\lambda + 1} \tag{3}$$

The coefficients C_1 to C_6 are C_1=0.5176; C_2=116; C_3=0.4; C_4=5; C_5=21; C_6=0.0068. The TSR is the ratio of the turbine blade linear speed to the wind speed

$$\lambda = \frac{\omega_t \mathrm{R}}{v_w} \tag{4}$$

where ω_t is the rotor blade tip speed in rad/s, and R is the radius of the turbine blade. The mechanical torque developed by the wind turbine is given as:

$$T_m = \frac{P_m}{\omega_t} = \frac{0.5 C_p(\lambda, \beta) \rho A v_w{}^3}{\omega_t} \tag{5}$$

The turbine power characteristics for different values of wind speeds and for the specified blade pitch angle (β) are shown in **Figure 1**:

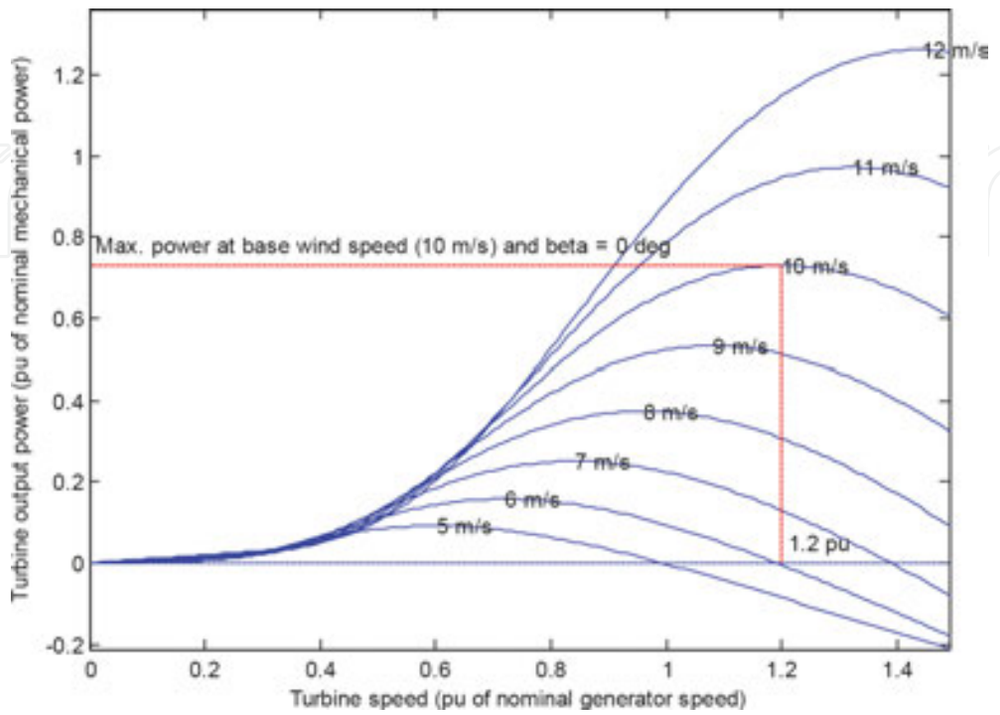


Figure 1. Turbine Power Characteristics for different values of wind speed.

3. The reluctance machine

Although reluctance machine has been known as early as induction machine, it has received minimal attention due to its relatively poor overall performance. Its earliest operations were largely in the motor mode for special applications [12, 13]. These applications include electric clocks, textile drives, synchronous switches drives, and the more sophisticated applications in nuclear reactors to position control rods with exact precision and reliability [14, 15]. However, since early 1960s, [14] and others started to study the theory and performance of poly-phase reluctance machines, and this paved way for an extensive study of the machine. Most of the studies carried out were however concentrated on the reluctance motor, until early 1980s when it was reported that the reluctance machine can also be operated as a SERG [16].

The reluctance machine is made up of a stator similar to that of the induction machine, and the rotor is basically a squirrel-cage induction machine rotor modified in order to have saliency in its magnetic circuit, which enhances the production of reluctance torque [14]. In order to ensure self-starting, the machine is provided with squirrel-cage rotor bars or damper cage windings. The principle of operation of the reluctance machine is based on the existence of varying air-gap reluctance, such that the opposition to the passage of magnetic flux is a minimum along an axis called the direct axis, and a maximum along an electrically perpen-

http://dx.doi.org/10.5772/62738

dicular axis, called the quadrature axis. The rotor is thus said to be magnetically anisotropic [15]. The tendency of the direct axis to align itself with the axis of the rotating magnetic field provided by the stator forms the basis for the operation of this machine.

Unlike induction machines, the motion of the rotor can be perfectly latched under the influence of the rotating magnetic field of the stator such that the rotor runs with the same speed of the stator's field. Thus, reluctance machine is a synchronous machine. This is a major advantage of the reluctance machine. Regardless of variations in the supply voltage and the load, the reluctance motor would run at synchronous speed. It is well-known that the output power of a reluctance machine increases with the ratio of the direct-axis inductance (or reactance) to the quadrature-axis inductance (or reactance) (L_d/L_q or X_d/X_q). Therefore, several attempts have been made to increase the L_d/L_q ratio [13]. To improve the overall performance of the reluctance machine, there have been improvements in electromagnetic designs which have brought about different rotor geometrical configurations. Because of these improved designs, the reluctance machine can compete favourably with the well-established induction machine [13]. Some of the rotor configurations include conventional salient pole rotor, segmented rotor, axially laminated anisotropic (ALA) rotor, flux-guided or flux-barrier rotor, and transversely laminated (TLA) rotor [13]. These have their different advantages and limitations.

3.1. Self-excited reluctance generator

The growing interest to harness renewable energy sources has informed the use of self-excited machines for energy conversion. Like the induction machine, the reluctance machine can also be used as a SERG driven by a prime mover. The self-excitation is initiated when suitable capacitors are connected across its stator terminals. As the rotor rotates, the residual flux in the rotor induces a small amount of electromotive force in the stator windings. With suitable capacitors connected across the stator terminals, a small amount of current flows in the stator windings which then increases the magnetic flux in the machine. The voltage then builds up in this manner until the magnetic core becomes saturated. Thus, these two conditions must be satisfied for self excitation and voltage build-up to occur [17]: (i) the rotor must have sufficient residual magnetism and (ii) the capacitance value must be adequate. The magnetizing inductance is a major factor for voltage buildup and stabilization of generated voltage for unloaded and loaded conditions.

4. Modelling of the self-excited reluctance generator

In this chapter, the following simplifying assumptions have been made.

i. Only the d-axis magnetizing inductance is affected by magnetic saturation.

ii. Core loss is negligible.

iii. Negligible space harmonics in the air-gap flux and time harmonics in the electromotive force and current waveforms.

4.1. Voltage equations

The equations of a reluctance machine can be obtained from those of the wound field synchronous machine with the field winding terms omitted [18, 19]. In rotor reference frame, the voltage equation for a synchronous reluctance generator with no rotor conductor can thus be written as follows:

$$v_{qs} = -r_s i_{qs} + \omega_r \lambda_{ds} + p\lambda_{qs} \tag{6}$$

$$v_{ds} = -r_s i_{ds} - \omega_r \lambda_{qs} + p\lambda_{ds} \tag{7}$$

$$\lambda_{qs} = -L_q i_{qs} \tag{8}$$

$$\lambda_{ds} = -L_d i_{ds} \tag{9}$$

$$L_q = L_{ls} + L_{mq} \tag{10}$$

$$L_d = L_{ls} + L_{md} \tag{11}$$

where: v_{qs} (v_{ds}) is the q-axis (d-axis) stator voltage, i_s is the stator current, r_s is the stator resistance, L_q (L_d) is the q-axis (d-axis) stator inductance, L_{mq} (L_{md}) is the q-axis (d-axis) stator mutual inductance, L_{ls} is the stator leakage inductance, λ_{qs} (λ_{ds}) is the q-axis (d-axis) stator flux linkage, ω_r is the rotor speed and p is the differential operator denoting $\frac{d}{dt}$.

The *q*-*d* equivalent circuit of the reluctance generator without a damper winding in the rotor as obtained from equations (6) to (9) is shown below. Since a generator is under consideration here, the direction of the stator current is taken to be out of the machine stator terminals.

4.2. Electromagnetic torque equation

The electromagnetic torque developed by the generator may be written as:

$$T_e = \left(\frac{3}{2}\right)\left(\frac{P}{2}\right)\left[\lambda_{ds} i_{qs} - \lambda_{qs} i_{ds}\right] \tag{12}$$

If we substitute (8) and (9) into (12), we obtain:

http://dx.doi.org/10.5772/62738

$$T_e = \left(\frac{3}{2}\right)\left(\frac{P}{2}\right)\left[\left(L_q - L_d\right) i_{qs} i_{ds}\right] \tag{13}$$

Where P is the number of poles on the SERG rotor. With the assumed current direction into the stator, this torque expression is positive for generator action and negative for motor action.

4.3. Coupling equation

A system of gears contained in a gearbox system is required to convert the lower rotational speeds on the wind turbine side to a high rotor speed on the generator side, for electrical energy production. The gear ratio is the ratio of the generator speed to the tip speed of the turbine blade.

Therefore, the coupling equation, which represents the swing equation of the generator is given as:

$$p\omega_r = \frac{P}{2J_T}\left(T_m - T_e - \frac{2}{P} B\omega_r\right) \tag{14}$$

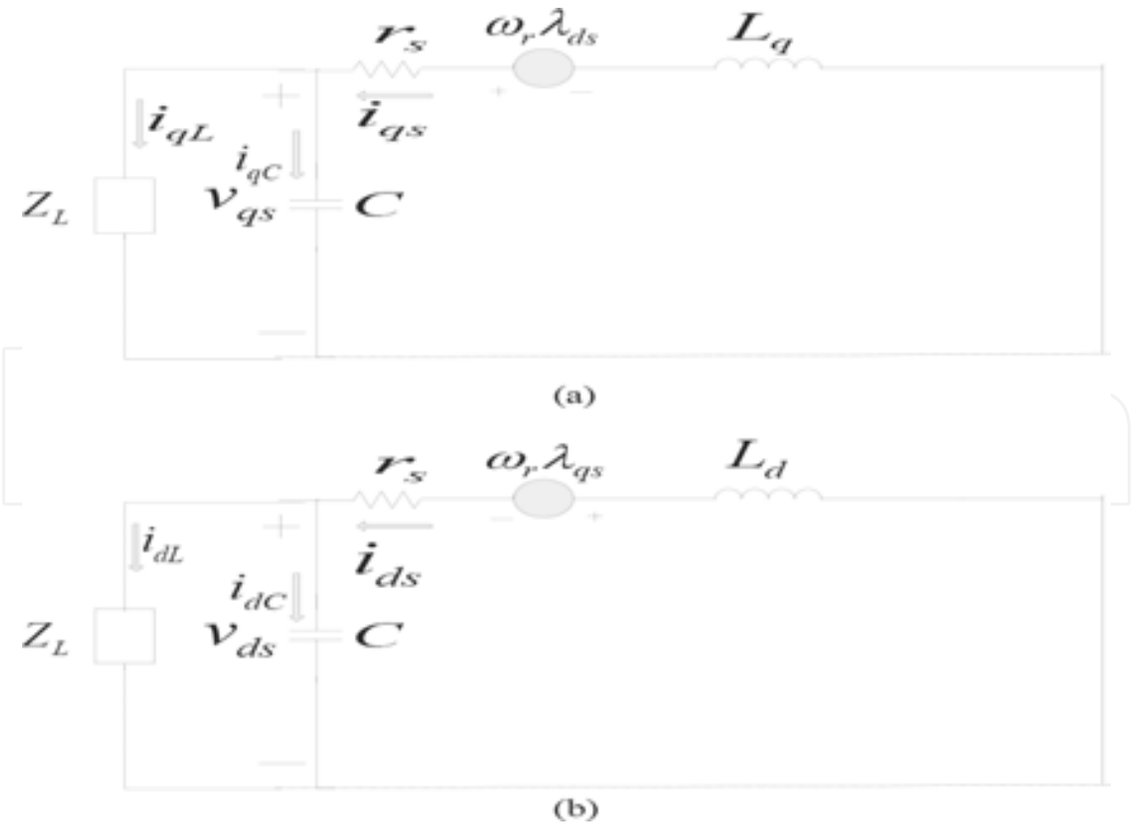


Figure 2. Rotor reference frame equivalent circuit of a self-excited reluctance generator. (a) q-axis (b) d-axis.

where B is the friction constant of the system. The wind turbine is represented as a single lumped inertia, J_T, in equation (14). This includes the inertial masses of the turbine blades, the gearbox, and the generator, referred to the generator side.

4.4. Excitation capacitance and load model

The stator terminals are connected to a capacitance bank in parallel with the load. The equations that relate the terminal voltages with the stator currents and load currents are presented in the following equations. Looking into the equivalent circuit of **Figure 2**, the nodal equation at the stator-capacitor-load terminals is obtained using Kirchoff's Current Law as:

$$i_{dC} = i_{ds} - i_{dL} \tag{15}$$

$$i_{qC} = i_{qs} - i_{qL} \tag{16}$$

i_{dC} (i_{qC}) and i_{dL} (i_{qL}) are the *d*-axis(*q*-axis) currents drawn by the excitation capacitors and the load respectively.

A general representation of the excitation capacitance in rotor reference frame is given in matrix form as:

$$\begin{bmatrix} i_{qC} \\ i_{dC} \end{bmatrix} = \begin{bmatrix} pC & \omega_r C \\ -\omega_r C & pC \end{bmatrix} \begin{bmatrix} V_{qL} \\ V_{dL} \end{bmatrix} \tag{17}$$

whereupon, the voltages are expressed as:

$$pV_{qL} = -\omega_r V_{dL} + \frac{i_{qs} - i_{qL}}{C} \tag{18}$$

$$pV_{dL} = \omega_r V_{qL} + \frac{i_{ds} - i_{dL}}{C} \tag{19}$$

Taking the load as a typical RLC, a general balanced RLC load model can be represented by:

$$V = iR + L\frac{di}{dt} + \frac{1}{C}\int idt \tag{20}$$

R_L , L_L , and C_L respectively represents the resistance, inductance, and capacitance of the load.

The RL load model can be obtained from (20) and it is expressed in rotor reference frame as:

http://dx.doi.org/10.5772/62738

$$i_{qL} = \int \frac{1}{L_L}\left[V_{qL} - i_{qL}R_L - \omega_r L_L i_{dL}\right]dt \tag{21}$$

$$i_{dL} = \int \frac{1}{L_L}\left[V_{dL} - i_{dL}R_L + \omega_r L_L i_{qL}\right]dt \tag{22}$$

5. Simulation of the WDSERG

A 2 hp (1.5 KW), 4-pole, 60 Hz machine with the parameters obtained from [20], and [21] is used for the simulation in this chapter. The parameters are given in **Table 1**.

Machine rating			**Tbase**	**Ibase(abc)**	r_s	L_q	**J**
Horsepower	Volts	Rpm	Nm	Amps	Ohms	H	Kgm^2
2	120	1800	7.9577	4.1667	3.77	0.081	0.1

Table 1. Reluctance machine parameters.

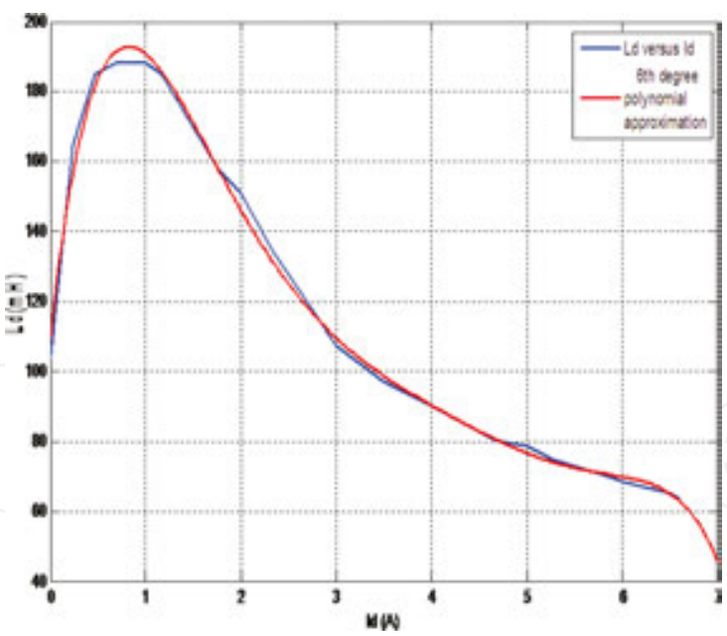


Figure 3. d-axis magnetising characteristic.

The magnetising characteristics of the machine is given by the L_d-I_d curve shown in **Figure 3**. A 6^{th} order curve fitting polynomial has been used to approximate the relationship. This enables the saturation effect to be taken into consideration.

The polynomial is given as:

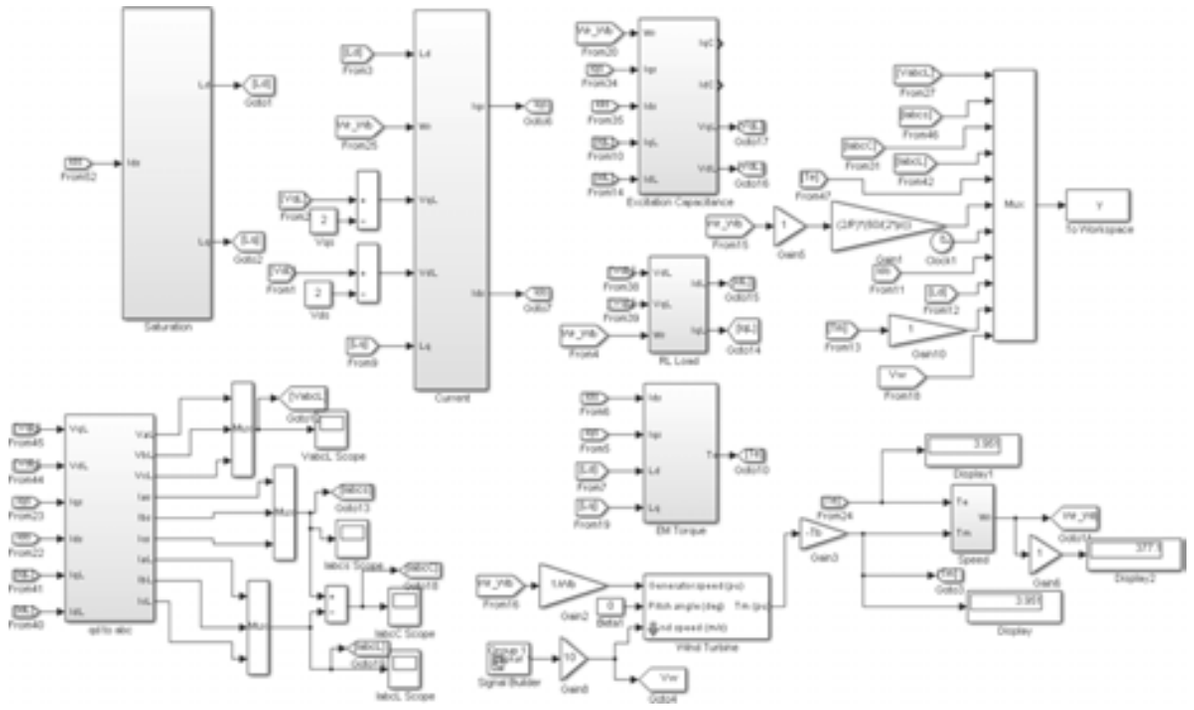


Figure 4. Complete WDSERG model in MATLAB-Simulink.

$$L_d = -0.10007 i_d{}^6 + 2.3788 i_d{}^5 - 22.52 i_d{}^4 + 107.06 i_d{}^3 - 259.15 i_d{}^2 + 253.62 i_d + 109.44 \tag{23}$$

5.1. MATLAB-Simulink implementation

The equations derived in the previous sections are arranged in forms suitable for simulation. For the purpose of clarity, the voltage equations have been rearranged below. By substituting equations (8) and (9) into (6) and (7) respectively, the currents can be expressed as:

$$i_{qs} = \frac{-\lambda_{qs}}{L_q} = -\int \frac{1}{L_q}\left[V_{qs} + r_s i_{qs} + \omega_r L_d i_d\right] dt \tag{24}$$

$$i_{ds} = \frac{-\lambda_{ds}}{L_d} = -\int \frac{1}{L_d}\left[V_{ds} + r_s i_{ds} - \omega_r L_q i_q\right] dt \tag{25}$$

The detailed MATLAB-Simulink model developed and utilised to simulate WDSERG is presented in the following **Figures 4** to **12**.

The model is made up of the different subsystems (saturation, current, excitation capacitance, EM torque, *qd* to *abc*, speed, wind turbine) as shown in **Figure 4**. The details in the saturation

http://dx.doi.org/10.5772/62738

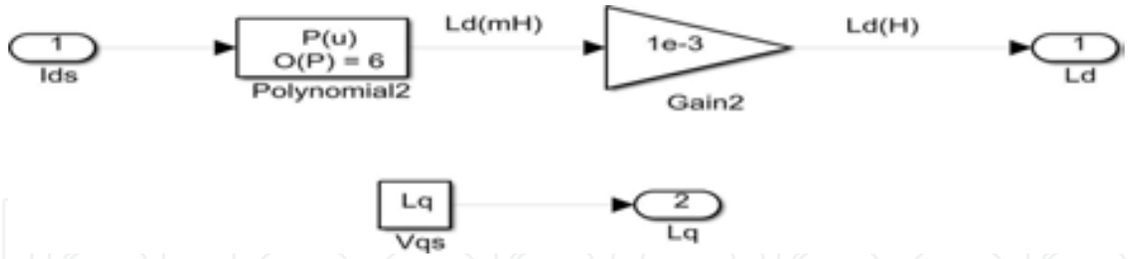


Figure 5. Saturation Subsystem.

subsystem is shown in **Figure 5**. This implements the magnetising characteristic approximated by equation (23), while **Figure 6** shows the details in the current subsystem and it implements equations (24) and (25). The shunt excitation capacitance is implemented by the details of the subsystem shown in **Figure 7**. The implementation of the RL load model derived from equations (21) and (22) is shown in **Figure 8**, while **Figures 9** and **10** respectively shows the electromagnetic torque and generator speed subsystems.

The inverse transformation (*qd* to *abc*) subsystem shown in **Figure 11** transforms the *qd* stator-load-capacitor terminal voltages, stator, capacitor, and load currents into machine (abc) variables. The wind turbine model in MATLAB-Simulink implementation is shown in **Figure 12**.

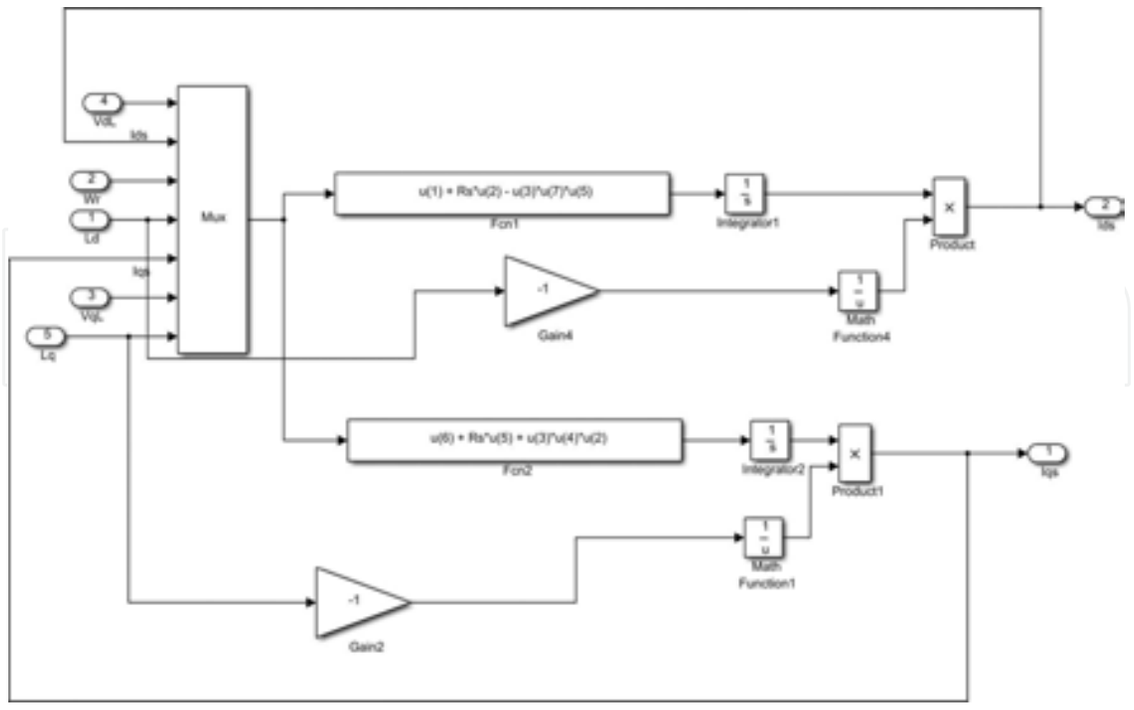


Figure 6. Current Subsystem.

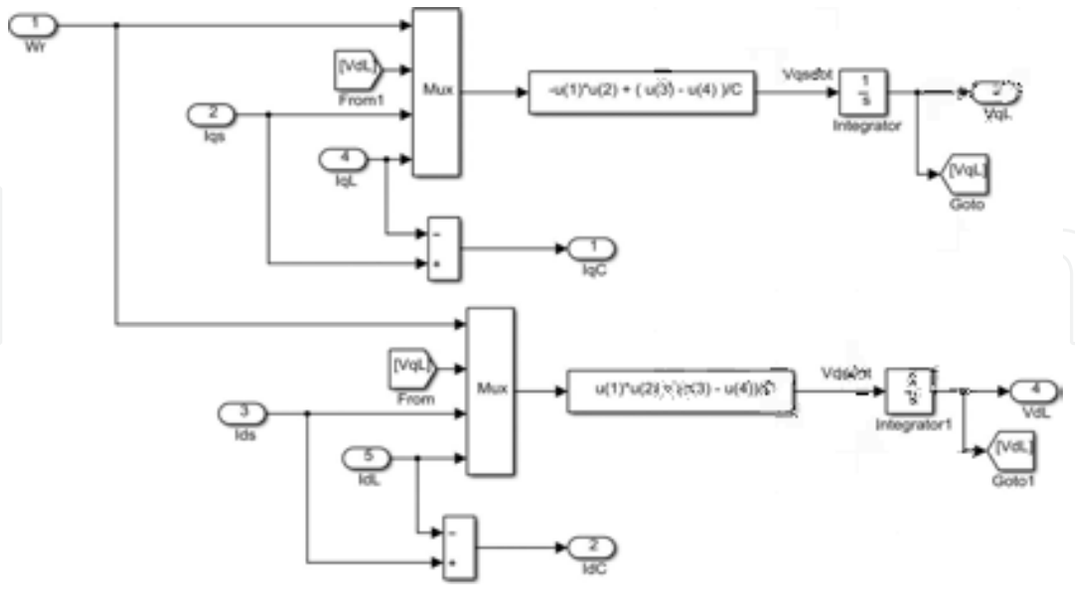


Figure 7. Shunt Excitation Capacitance Subsystem.

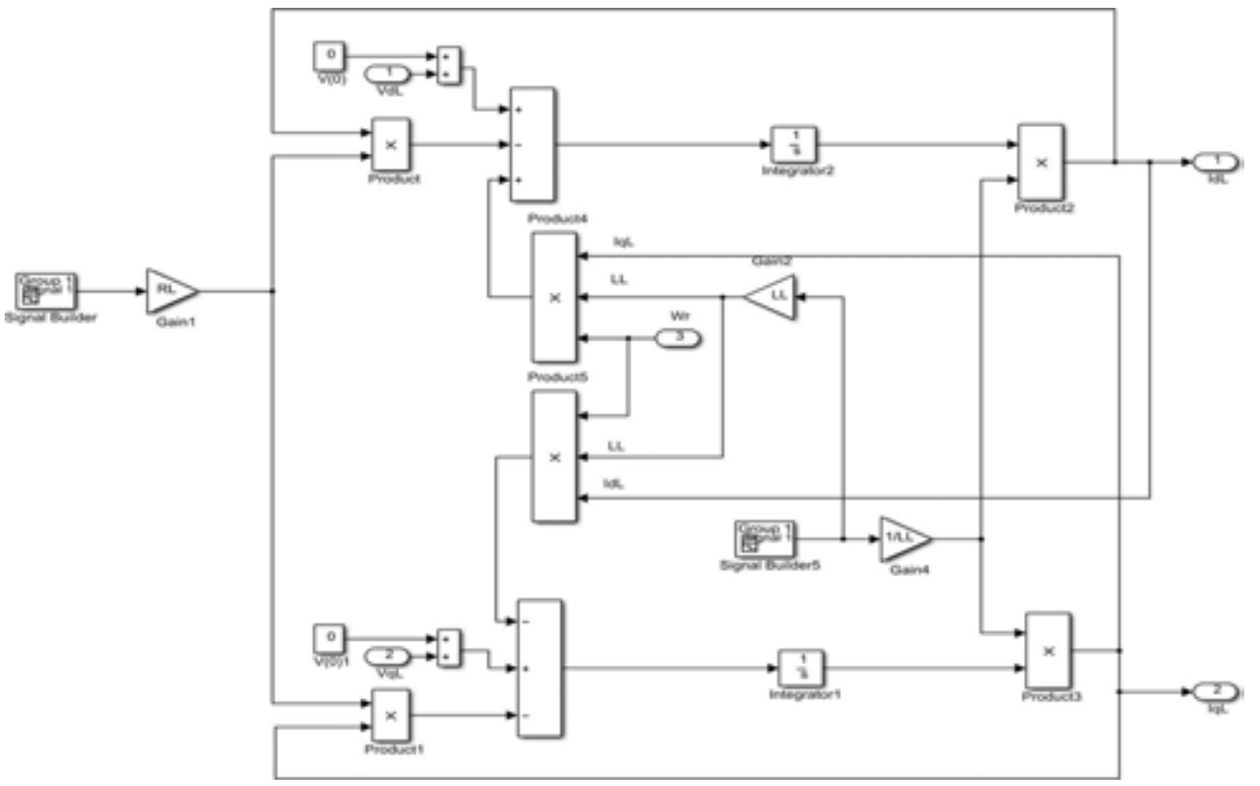


Figure 8. RL Load Subsystem.

http://dx.doi.org/10.5772/62738

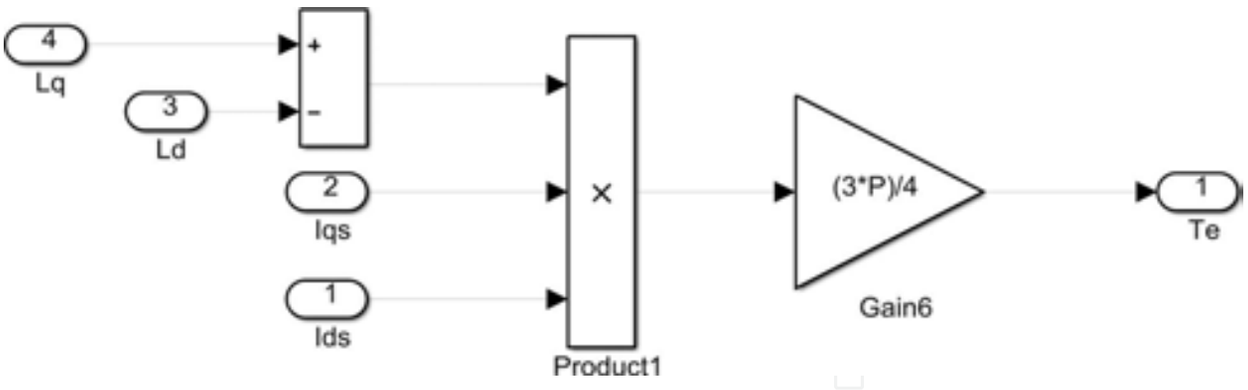


Figure 9. Electromagnetic Torque Subsystem.

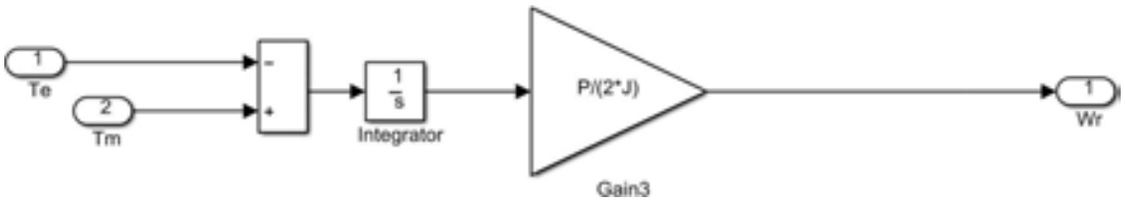


Figure 10. Rotor Speed Subsystem.

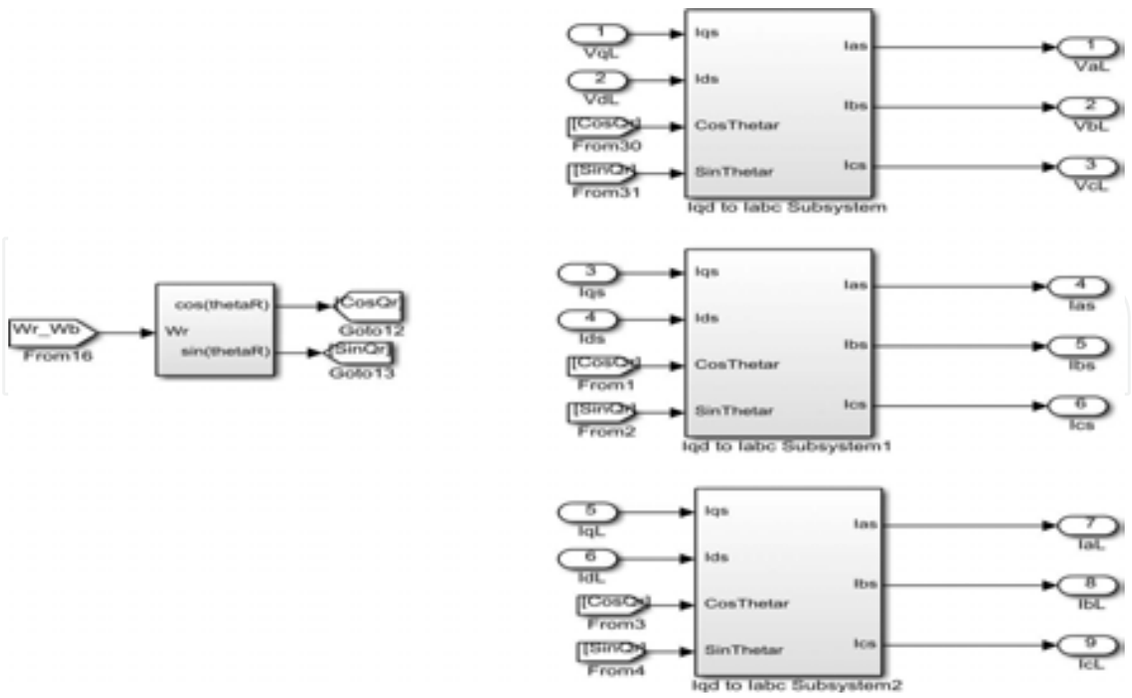


Figure 11. *qd* to *abc* subsystem.

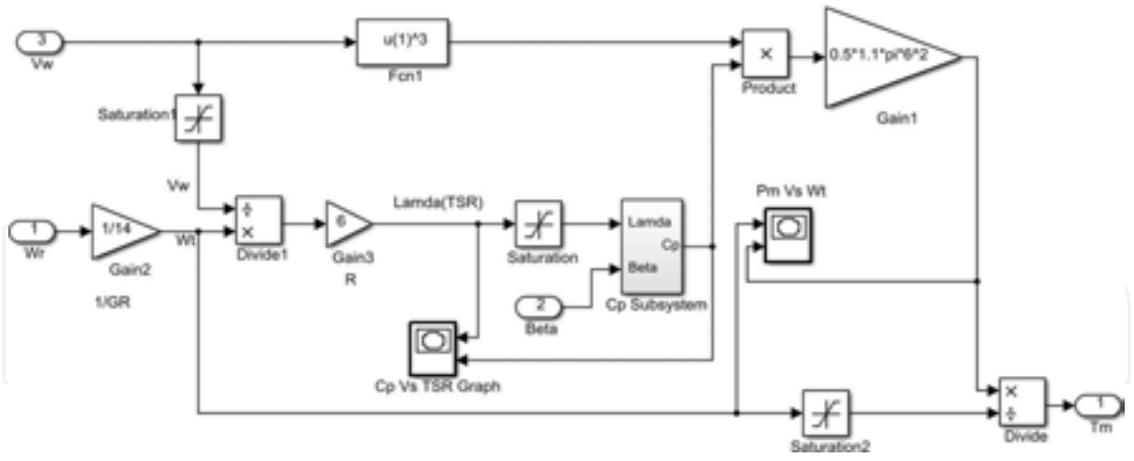


Figure 12. Wind Turbine Model.

6. Simulation result

The simulation has been done using MATLAB-Simulink to observe the performance of the system under the following conditions:

a. Constant wind speed

b. Wind Speed Variation

c. Load variations

The stator terminals are connected to a balanced star-connected capacitance bank of $85\mu F$ per phase. It has been mentioned earlier, that for a successful excitation and voltage build up, there must be a sufficient residual emf. This has been represented in the simulink model by an assumed value of 2 V.

A no load condition can be simulated using a very large value of R and L (**Figure 13**). Under this condition, the terminal impedance is so high that it can be regarded as an open circuit. The result of the simulation under this condition is shown in **Figure 13**. The stator phase current is about 10.33 A, while the load current is practically equal to zero (0.000035 A). The electromagnetic torque developed, which is equal to the wind turbine torque rises to a steady value of 3.707 Nm.

6.1. WDSERG performance at constant wind speed

The performance of the WDSERG under a constant wind speed of 10 m/s and an RL load (R = 400 Ohms; L = 30 mH) is shown in **Figure 14**. The wind turbine torque rose to a steady value of 0.7611 Nm. As the wind torque is applied, the generator speed quickly rises to the synchronous speed of 1800 rpm. The electromagnetic torque developed by the machine closely matches the wind torque, which invariably leads to a constant SERG speed.

http://dx.doi.org/10.5772/62738

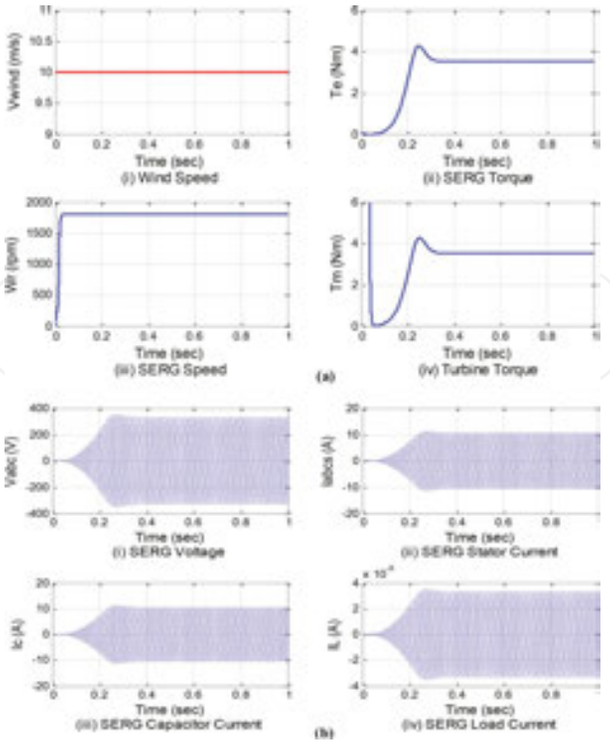


Figure 13. WDSERG At Vwind = 10m/s at No load (R = 10Megaohms; L = 30H).

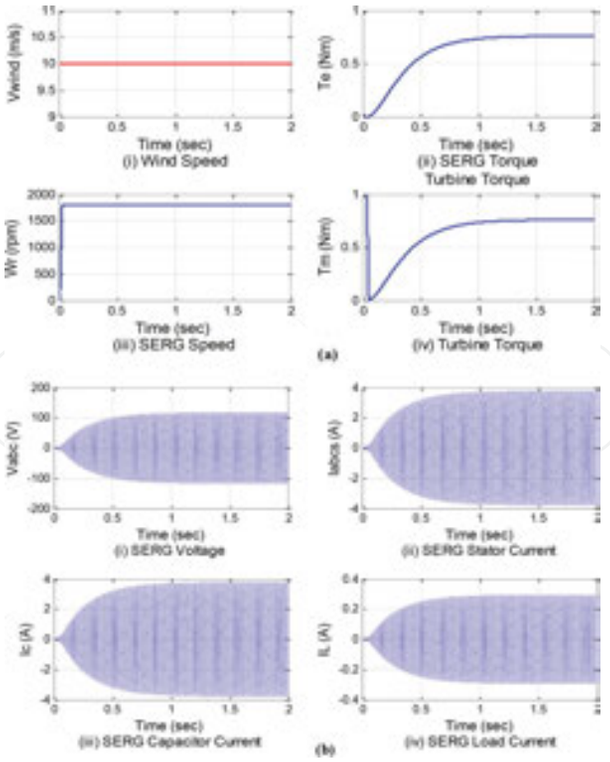


Figure 14. WDSERG At Vwind = 10m/s with R = 400ohms; L = 30mH.

It is observed that a WDSERG would perform smoothly with a constant wind speed profile.

6.2. WDSERG performance at varying wind speed

This scenario is analysed in two possible cases of decrease in wind speed and increase in wind speed as follows:

6.2.1. Decrease in wind speed

The dynamic response of the wind-driven SERG when the wind speed suddenly falls to 8 m/s for an RL load of 400 Ohms, 30 mH. The wind torque and the electromagnetic torque also falls suddenly from an initial value of 0.7611 Nm to a value of 0.3656 Nm. As the wind speed falls, the generator speed also falls from the synchronous value of 377 rad/s (1800 rpm) to 301.9 rad/s (1441.5 rpm).

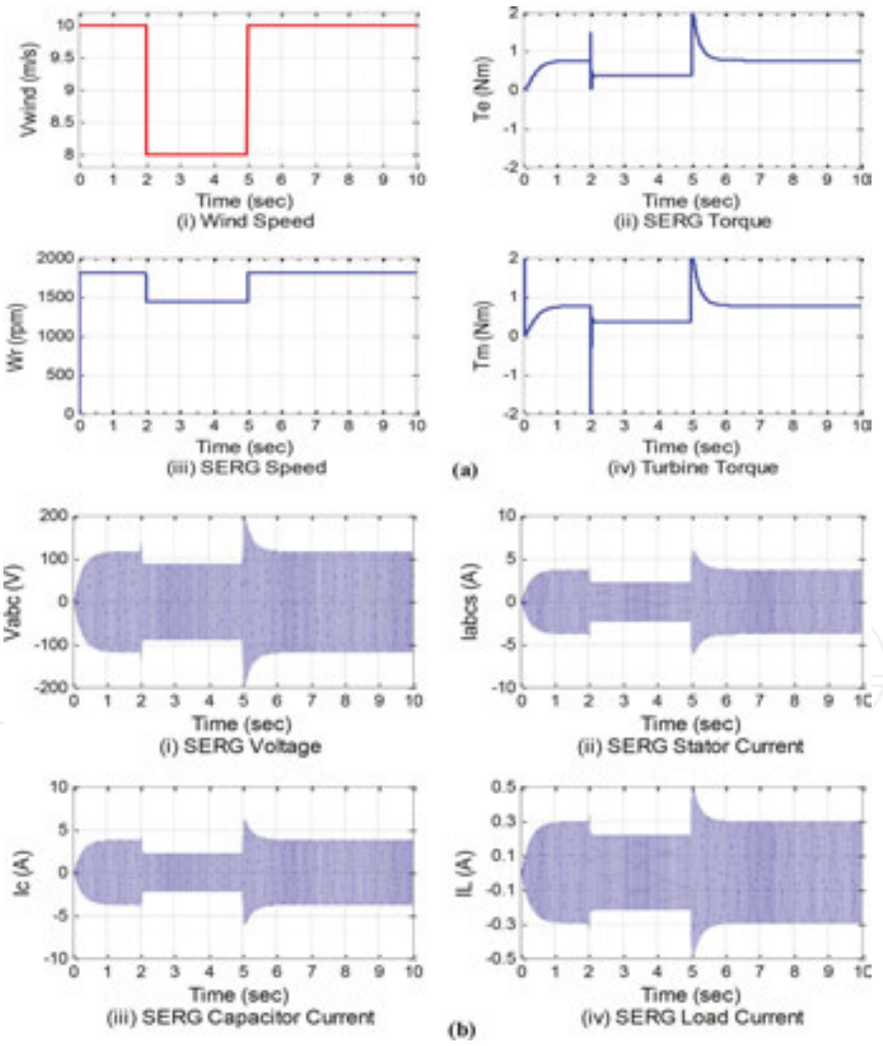


Figure 15. Dynamic response of the WDSERG when the wind speed suddenly falls to 8m/s.

http://dx.doi.org/10.5772/62738

Under this input condition, the generated voltage falls from a value of 118 V to a new value of about 100 V. The machine continues in this new values until 5 s when the wind speed was suddenly returned to 10 m/s. Thus, a decrease in the wind speed tends to reduce the generated voltage (**Figure 15**).

6.2.2. Increase in wind speed

In **Figure 16**, with an RL load of 400 Ohms, 30 mH, and an excitation capacitance of $85\mu F$, the wind speed is suddenly increased to a value of 10.2 m/s at 2 s and then dropped back to 10 m/s at 4 s. The figure shows that as the wind speed is increased by this small value, the generated voltage suddenly falls from a value of 118 V to about 25 V. This shows that in this particular case, the generated voltage of the wind-driven SERG tends to collapse at an increased wind speed. For the value of $85\mu F$ excitation capacitance, the SERG could not be operated with a

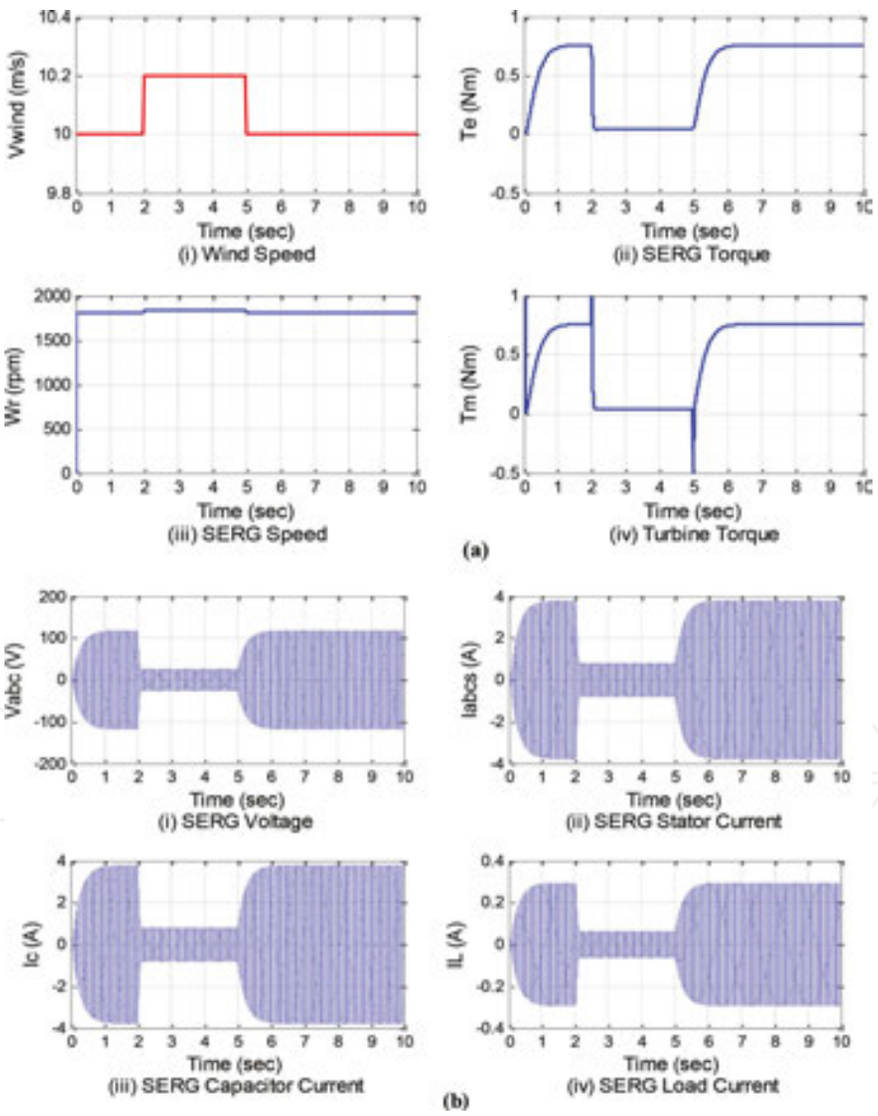


Figure 16. Dynamic response of the WDSERG when the wind speed suddenly rises to 10.2m/s.

reasonable voltage build up at wind speeds above 10 m/s, as this produces a generator speed greater than the rated synchronous speed. However, a reasonable voltage build-up is observed when the excitation capacitance is reduced accordingly. This shows that the excitation capacitance requirement reduces as the wind speed increases. This result therefore shows an inverse relationship between excitation capacitance and rotor speed. For $85\mu F$ excitation capacitance, **Figure 16** shows the wind torque and the electromagnetic torque falling to a very low value (0.041 Nm) at 2 s when the wind speed rises to 10.2 m/s and the torque rises again at 4 s when the wind speed decreases sharply back to 10 m/s to attain the initial steady value of 0.7611 Nm. However, at a selected lower capacitance value, the WDSERG voltage builds up appreciably at 12 m/s. Thus, a well-designed pitch-control mechanism for the wind turbine is necessary to operate the WDSERG at higher wind speeds with a fixed excitation capacitance, such that the torque developed by the wind speed is not above the value required to drive the generator at rated speed. Alternatively, the SERG can be provided with wind-following excitation.

6.3. SERG performance under load variations

A scenario of an overloaded condition was simulated using an effective load impedance which reduced in steps from 400 Ohms to 200 Ohms at 2 s to 100 Ohms at 4s then to 80 Ohms at 6 s and finally back to 400 Ohms. The result of the simulation is illustrated in **Figure 17**. It is observed that at t = 2s, when the load suddenly changes to 200 Ohms, there is a remarkable fall in the voltage level. The generated voltage continues to fall at 4 s and at 6 s until it rapidly falls toward zero as a result of overload. This illustrates that at an overloaded condition, the generator will suffer voltage collapse. The voltage builds up again at 8 s when the load changes back to its initial impedance value.

The performance of the WDSERG under varying loads is shown in **Figure 18**. When the RL load suddenly changes from 400 Ohms, 35 mH to 300 Ohms, 105 mH at 3 s, and then changes back to the initial RL values at 6 s, the following are observed:

(a) At 3 s, the drive torque and hence the electromagnetic torque falls from a value of 0.8216 Nm to a new steady state value of 0.6181 Nm. This consequently leads to a reduction in both the stator voltages and currents. The voltage dropped from about 123 V to a steady value of 101 V, and the stator current falls from about 4 A to about 3.2 A. However, during this period the load current increases slightly due to an increase in load inductance. When the RL value is suddenly increased again at 6 s, the voltage and current rises back to their initial values.

In spite of the sudden increase and decrease in the load, the speed of the SERG remains constant at 1800 rpm, and hence the frequency. Thus, there is a constant output frequency regardless of the variations in load. This is unlike the SEIG, whose voltages and frequency are heavily affected by varying loading conditions [22]. It is obvious also that though the WDSERG voltage output varies with the load, this variation may not be as severe compared to the SEIG.

http://dx.doi.org/10.5772/62738

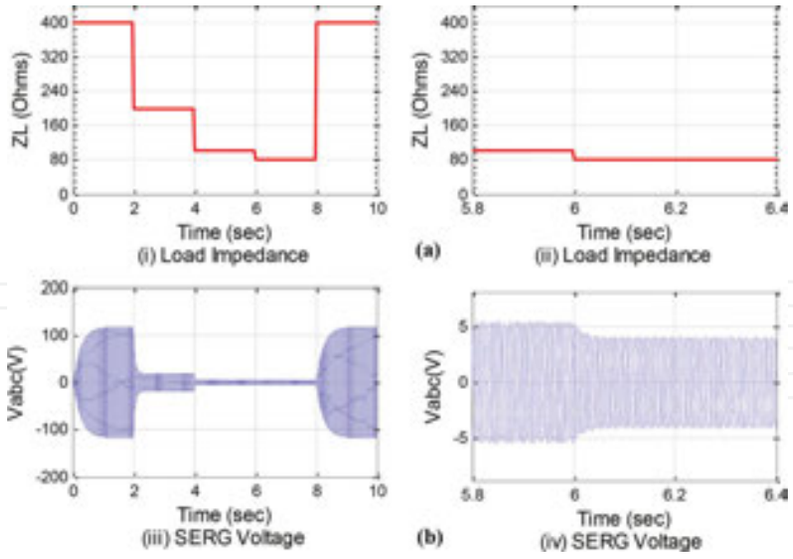


Figure 17. Voltage Collapse of the WDSERG.

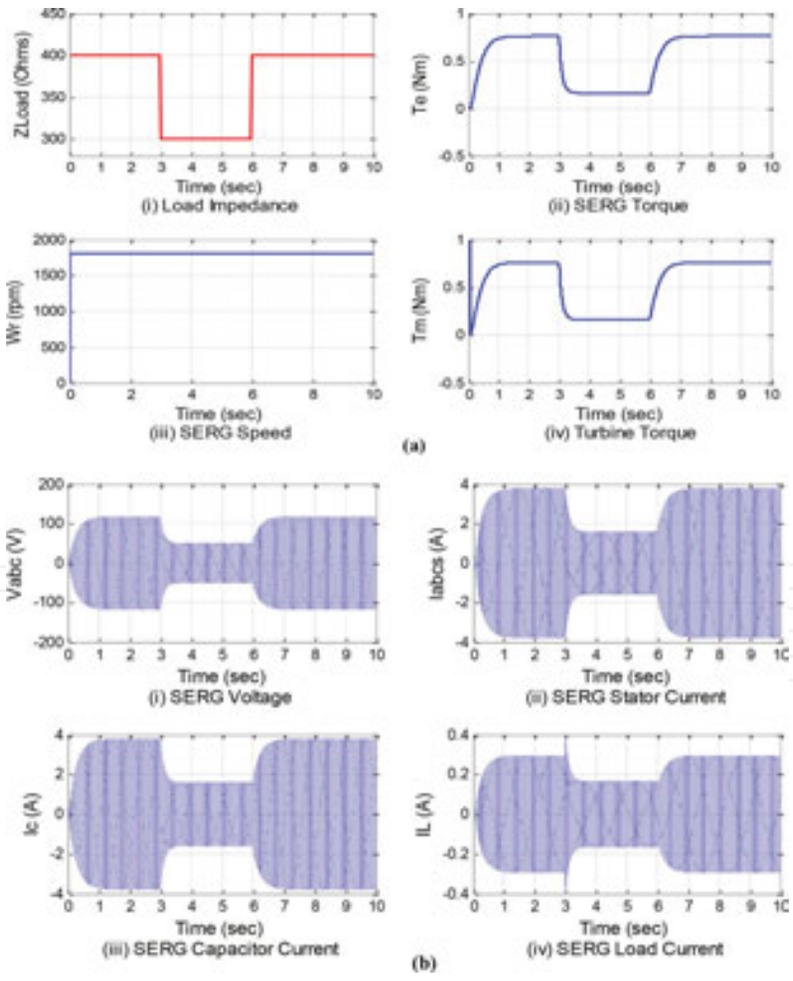


Figure 18. Dynamic response of the WDSERG under sudden increase and decrease in the RL load at Vwind = 10m/s.

7. Conclusion

The dynamic performance of a wind-driven SERG has been analysed and presented under conditions of constant wind speed, varying wind speed, and varying load. A step-by-step procedure for the MATLAB-Simulink implementation has been clearly presented.The results show that the generated voltage slightly falls with increasing load, and requires an increase in excitation capacitance within the stable operating limits to maintain a constant generated voltage. A wind-driven SERG will however operate at constant output frequency regardless of the load variations at its output terminals. This makes the SERG a good candidate for wind power application in rural electrification.

Author details

Ayodeji S.O. Ogunjuyigbe[1*], Temitope R. Ayodele[1], Bukola B. Adetokun[1] and Adisa A. Jimoh[2]

*Address all correspondence to: a.ogunjuyigbe@ui.edu.ng

1 Power Energy Machines and Drives (PEMD) Research Group, Department of Electrical and Electronic Engineering, University of Ibadan, Nigeria

2 Electrical Engineering Department, Tshwane University of Technology, Pretoria, South Africa

References

[1] T. R. Ayodele and A. S. O. Ogunjuyigbe, "Wind energy resource, wind energy conversion system modelling and integration: a survey," *International Journal of Sustainable Energy,* vol. 34, pp. 657–671, 2015.

[2] N. H. Malik and S. E. Haque, "Steady state analysis of an isolated self-excited induction generator," *IEEE Transactions on Energy Conversion,* vol. 1, pp. 133–139, 1986.

[3] K. Idjadarene, D. Rekioua (ZIANI), T. Rekioua, and A. Tounzi, "Performance of an isolated induction generator under unbalanced loads," *IEEE Transactions on Energy Conversion,* vol. 25, 2010.

[4] T. R. Ayodele, A. S. O. Ogunjuyigbe, and O. O. Akinola, "Optimal location, sizing, and appropriate technology selection of distributed generators for minimising power loss using genetic algorithm," *Journal of Renewable Energy,* vol. 2015, pp. 1–9, 2015.

[5] A. I. Alolah, "Capacitance requirements for three-phase self-excited reluctance generator," *IEE Proceedings on Generation, Transmission and Distribution,* vol. 138, pp. 193–198, 1991.

[6] S. C. Kuo and L. Wang, "Analysis of isolated self-excited induction generator," *IEEE Proceedings on Generation, Transmission and Distribution,* vol. 149, pp. 90–97, 2002.

[7] Y. H. A. Rahim, J. E. Fletcher, and N. E. A. M. Hassanain, "Performance analysis of salient-pole self-excited reluctance generators using a simplified model," *IET Renewable Power Generation,* vol. 4, pp. 253–260, 2010.

[8] F. M. El-Khouly and A. M. Osheiba, "Brushless induction and reluctance generators with DC excitation: experimental verification," *Electric Power Components and Systems,* vol. 32, pp. 839–853, 2004.

[9] W. S. Abu-Elhaija, "Capacitance requirement of single-phase self-excited reluctance generator using eigenvalues criterion," in *Proceedings on IEEE PES Transmission and Distribution Conference & Exposition (TD 2005-000019)*, Dallas, Texas, pp. 21–25, 2006.

[10] A. L. Mohamadein, Y. H. A. Rahim, and A. S. Al-Khalaf, "Steady state performance of self-excited reluctance generators," in *IEE Proceedings on Electric Power Apparatus*, 293–298, 1990.

[11] O. O. Mengi and I. H. Altas, "Fuzzy logic control for a wind/battery renewable energy production system," *Turkish Journal of Electrical Engineering & Computer Sciences,* vol. 20, 2012.

[12] M. H. Nagrial and M. A. Rahman, "Operation and characteristics of self-excited reluctance generator," in *Proceedings of IEEEIAS Annual Meeting*, 55–58, 1988.

[13] A. S. O. Ogunjuyigbe and A. A. Jimoh, "On the development and performance of reluctance machine," *International Review of Automatic Control (I.RE.A.CO),* vol. 5, 316–326, 2012.

[14] P. J. Lawrenson and L. A. Agu, "Theory and performance of polyphase reluctance machines," *Proceedings of IEE,* vol. 111, 1435–1445, 1964.

[15] L. U. Anih, E. S. Obe, and S. E. Abonyi, "Modelling and performance of a hybrid synchronous reluctance machine with adjustable Xd/Xq ratio," *IET Electric Power Applications,* vol. 9, 171–182, 2015.

[16] F. E. Abdel-Kader, "The reluctance machine as a self-excited generator," *Electric Machines and Power Systems,* vol. 10, 141–148, 1985.

[17] A. Kishore, R. C. Prasad, and B. M. Karan, "MATLAB SIMULINK based DQ modeling and dynamic characteristics of three phase self excited induction generator," in *Progress in Electromagnetics Research Symposium*, Cambridge, USA, 312–316, 2006.

[18] P. Krause, O. Wasynczuck, and S. Sudhoff, *Analysis of Electric Machinery and Drive System*, John Wiley & Son Publication, 2002.

[19] D. W. Novotny and T. A. Lipo, *Vector Control and Dynamics of AC Drives,* Clarendon Press, Oxford, 1996.

[20] I. Boldea, Z. X. Fu, and S. A. Nasar, "High-performance reluctance generator," in *IEE Proceedings-B*, 124–130, 1993.

[21] M. Enache, C. Nica, and S. Ivanov, "Aspects regarding modelling of reluctance synchronous motors," in *6th International Conference on Electromechanical and Power Systems*, Chisinau, Rep. Moldova, 126–129, 2007.

[22] L. Wang and Y. Wang, "Characteristics of a self-excited reluctance generator as affected by sudden connection and disconnection of an induction motor load," in *IEEE International Conference on Power System Technology*, 1998.

IntechOpen